Earth Surface Processes and Landforms
Earth Surf. Process. Landforms **33**, 890–909 (2008)
Published online in 11 September 2007 Wiley InterScience
(www.interscience.wiley.com) **DOI:** 10.1002/esp.1581

Modeling fluvial response to in-stream woody vegetation: implications for stream corridor restoration

Sean J. Bennett,[1]* Weiming Wu,[2] Carlos V. Alonso[3] and Sam S. Y. Wang[2]
[1] *Department of Geography, University at Buffalo, Buffalo, NY, USA*
[2] *National Center for Computational Hydroscience and Engineering, The University of Mississippi, MS, USA*
[3] *USDA-ARS National Sedimentation Laboratory, Oxford, MS, USA*

**Correspondence to: Sean J. Bennett, Department of Geography, University at Buffalo, Buffalo, NY 14261-0055, USA. E-mail: seanb@buffalo.edu*

Received 31 January 2007;
Revised 20 June 2007;
Accepted 26 June 2007

Abstract

River restoration and bank stabilization programs often use vegetation for improving stream corridor habitat, aesthetic and function. Yet no study has examined the use of managed vegetation plantings to transform a straight, degraded stream corridor into an ecologically functional meandering channel. Experimental data collected using a distorted Froude-scaled flume analysis show that channel expansion and widening, thalweg meandering and riffle and pool development are possible using discrete plantings of rigid, emergent vegetation, and the magnitudes of these adjustments depend on the shape of the vegetation zone and the density of the vegetation. These experimental results were verified and validated using a recently developed numerical model, and model output was then used to discuss mechanistically how rivers respond to the introduction of in-stream woody vegetation. Finally, a hybrid method of meander design is proposed herein where managed vegetation plantings are used to trigger or force the desired morphologic response, transforming a straight, degraded reach into a more functional meandering corridor. It is envisioned that such numerical models could become the primary tool for designing future stream restoration programs involving vegetation and assessing the long-term stability of such activities.

Keywords: stream restoration; riparian vegetation; physical model; numerical model; river meandering

Introduction

Stream restoration or rehabilitation programs seek to return a degraded aquatic or riparian ecosystem to its remaining natural potential rather than its pre-disturbed condition, as measured by key indices such as habitat quality, biodiversity and ecologic integrity (US EPA, 2000a, 2000b; Shields *et al.*, 2003; Wohl *et al.*, 2005). In the US, stream restoration programs seek most commonly to enhance water quality, to manage riparian zones, to improve in-stream habitat and fish passage and to stabilize stream banks, and these activities cost in excess of $1B per year (Bernhardt *et al.*, 2005). For regions such as Mississippi and the Loess Belt of the south–central US, degraded or impaired streams are characterized by flashy hydrographs, steep and unstable banks, excessive sediment loads, straight, incised and relatively wide channels, shallow baseflows and denuded riparian zones (Shields *et al.*, 1995a, 1995b; Thorne, 1999; Simon and Rinaldi, 2000). Recent discussions have focused on identifying tools and technology for channel reconstruction (Shields *et al.*, 2003), defining conceptually the science of river restoration (Wohl *et al.*, 2005), proposing ecologic criteria for assessing the success of restoration programs (Palmer *et al.*, 2005) and addressing current limitations of restoration activities (Hilderbrand *et al.*, 2005; Wohl *et al.*, 2005). There is a clear movement amongst researchers and practitioners to more effectively meld river mechanics and fluvial geomorphology with ecology (Palmer and Bernhardt, 2006).

To achieve these goals, stream restoration and bank stabilization programs have embraced the use of vegetation. These techniques include managed plantings of grasses, live cuttings or dormant posts, combinations of rocks, revetments

and vegetation, and engineered log jams and woody debris (see, e.g., USDA-NRCS, 1996; FISRWG, 1998; Abbe *et al.*, 2003; Shields *et al.*, 2004). While this vegetation provides ecologic benefits to river corridors in terms of habitat, habitat resources and physical complexity, the practitioner clearly is exploiting the effects vegetation has on stream flow to achieve the desired goal. Because it is a local sink for fluid momentum, vegetation suppresses near-bed velocity gradients and Reynolds stresses within the canopy, it induces sediment deposition and it increases total flow resistance in rivers with vegetated boundaries (Petryk and Bosmajian, 1975; Hupp, 2000; Nepf and Vivoni, 2000; López and García, 2001). The magnitude of these effects depends on the characteristics of the vegetation such as diameter, shape, flexibility, orientation, concentration or density, and relative submergence. Thus by markedly decelerating flow and shear stresses within the flow the introduction of vegetation to stream corridors can induce local deposition of sediment while affording protection to stream banks and beds from hydraulic attack. Here, the vegetation is viewed in the traditional way: it is a passive agent for river channel change. Recent work now suggests that vegetation exploits ecologic and geomorphic opportunities and can effectively engineer entire river corridors and exert tremendous influence on river form, process and sediment deposition (Johnson, 2000; Piégay *et al.*, 2000; Gurnell *et al.*, 2006; Gurnell and Petts, 2006).

Transforming and restoring a straight, degraded stream channel into a meandering channel through the use of vegetation should enhance greatly the ecologic functionality and physical complexity of the corridor, cause local bar and pool development and provide local protection to stream banks and beds. This approach to stream corridor restoration was first proposed by Bennett *et al.* (2002). Using an experimental channel, Bennett *et al.* (2002) showed that a straight, degraded stream channel could adopt a meandering thalweg, therein defined as the location of maximum surface velocity, by introducing rigid, emergent vegetation at the prescribed spacing of equilibrium meander beds based on flow discharge. At the highest density, and in comparison to the unvegetated channel, the introduced vegetation caused severe flow deceleration within and upstream of the zone, caused flow acceleration around the zone and the deflection of flow toward the outer bank, and caused thalweg meandering. The wavelength of the thalweg was equal to that of the vegetation zones, but its amplitude increased with vegetation density. The potential field application of these results was somewhat limited because the bed and banks of the flume were fixed (non-adjustable). Wu and Wang (2004a) successfully simulated this experimental flow field using a depth-averaged two-dimensional (2D) numerical model.

While many studies have discussed the effects of riparian vegetation on flow, sediment transport, and channel form in rivers (see Hupp and Osterkamp, 1996; Tsujimoto, 1999; Montgomery and Piégay, 2003; Bennett and Simon, 2004; Hupp and Rinaldi, 2007), none has utilized vegetation for the purpose of inducing a straight, degraded stream to meander. The goal of the current research program was to demonstrate the efficacy of using managed plantings of vegetation for stream corridor restoration and to develop a numerical and theoretical framework for modeling stream channel adjustment to vegetation. The objectives of the present study were (1) to systematically vegetate a straight, degraded experimental channel with freely adjustable banks and bed and to document the effects of vegetation density on alluvial response and channel morphology and (2) to compare these experimental results with a recently developed numerical model capable of simulating flow, sediment transport and bed morphology in meandering streams with riparian and in-stream vegetation. It is envisioned that, once validated, such numerical models could be used by the practitioner to design stream restoration and bank stabilization programs involving the use of vegetation and to assess the long-term efficacy and stability of such activities.

Experimental and Numerical Methods

Physical model design

In a companion study, Wallerstein *et al.* (2001) examined in detail the response of an experimental stream corridor to the introduction of large woody debris (LWD) of various configurations. This was accomplished by constructing a distorted Froude-scale physical model for a designated prototype, Abiaca Creek in northern Mississippi, USA, which is characterized by the widespread occurrence of LWD at various geomorphic positions within its basin (Wallerstein and Thorne, 2004). Channel dimensions for the two-year return flow Q_B for the prototypical reach along Abiaca Creek are presented in Table I. The basis for physical models in general is discussed by Henderson (1966) and Julien (2002), whereas the derivation, justification, and necessary distortions of the current model are discussed by Wallerstein *et al.* (2001) and only briefly summarized below.

The approach commonly adopted in physical-scale laboratory models is to ensure Froude number Fr similarity between field prototype (subscript p) and model (subscript m), such that their ratio (subscript r) is equal to unity:

$$Fr_r = \frac{Fr_p}{Fr_m} = \frac{u_r}{\sqrt{g_r d_r}} = 1 \tag{1}$$

DOI: 10.1002/esp

Table I. Summary of field conditions for Abiaca Creek, MS (prototype) and the distorted Froude-scaled flume model of Wallerstein *et al.* (2001) and the present study

Parameter	Prototype Abiaca Creek, MS	Wallerstein *et al.* (2001) model	This study
w_T (m)	17·9	0·3	0·312
w_B (m)	NA	0·1	0·1
L (m)	65·0	1·0	5·0
Q_B ($m^3 s^{-1}$)	48·1	0·0033	0·0033
d (m)	1·9	0·07	0·069
u (m)	1·4	0·24	0·232
S	0·011	0·0022	0·0019
D (mm)	0·25	0·8	0·8
u_* ($m s^{-1}$)	0·13	0·029	0·030
θ	4·17	0·065	0·070
Fr	0·32	0·29	0·28
D_v (m)	1·1	0·019	0·005

$\theta = \rho u_*^2/(\sigma - \rho)gD$ where θ is dimensionless shear stress and σ is sediment density. All other variables are defined in the text.

where u is the mean downstream flow velocity, g is gravitational acceleration, $g_r = 1$ and d is flow depth. Similarity of the flow conditions is maintained if the Reynolds number Re is sufficiently high to ensure fully turbulent flow in the model ($Re \geq 1400$), defined as

$$Re = \frac{\rho u^2}{\mu u/d} \tag{2}$$

where ρ and μ are the fluid's density and molecular viscosity, respectively. Although highly desirable, complete similarity between model and prototype, that is geometric, kinematic and dynamic similitude, is difficult to scale for movable-bed models given the physical dimensions of laboratory channels (Henderson, 1966; Wallerstein *et al.*, 2001; Julien, 2002). Limitations of this approach, in light of these distortions and the results obtained, are discussed below.

The physical model used herein needed to satisfy the following dimensional and hydraulic conditions. First, the bed and banks of the model needed to be freely adjustable, thus the entire stream corridor could respond to the introduced vegetation. Second, the sediment of the channel boundary needed to be just below the threshold of motion at the bankfull or channel-forming discharge Q_B of the prototype, and these threshold conditions were determined experimentally. This requirement ensured that the channel was stable with uniform roughness prior to the vegetation plantings and all subsequent alluvial channel adjustment was the direct result of the vegetation and its impact on the flow. Finally, the model would be constructed in a tilting, recirculating flume 0·63 m wide. Thus, the top width of the model w_T was fixed at 0·312 m to allow for sufficient lateral adjustment (bank erosion) during the test runs.

Given these constraints, using a grain size D of 0·8 mm, and the bankfull dimensions of the prototype, a distorted Froude-scaled flume model was constructed having a trapezoidal channel cross-section with a top width w_T of 0·312 m, a bottom width w_B of 0·1 m and 33° bank sideslopes. At a bankfull condition Q_B of 0·0033 $m^3 s^{-1}$ and channel bed slope S of 0·0019, a steady, uniform flow just below the threshold of sediment movement and bank instability was attained with a spatially averaged flow velocity u of 0·232 m s^{-1}, centerline flow depth d of 0·069 m, spatially averaged shear velocity u_* of 0·030 m s^{-1}, where $u_* = \sqrt{gRS}$ and R is hydraulic radius, and a Froude number Fr of 0·28. The model dimensions and bulk hydraulic conditions used herein were nearly identical to those used previously by Wallerstein *et al.* (2001; Table I).

Experimental apparatus and procedure

The experiments were conducted in a tilting, recirculating flume 0·63 m wide, 0·61 m deep and 10 m long. The channel was filled with 0·8 mm diameter sediment D to a depth of 0·5 m. After pre-wetting the sand, a trapezoidal channel with a top width w_T of 0·312 m, a bottom width w_B of 0·1 m and a reach length L of 5 m was cut into the sediment using a aluminum plate mounted on a movable carriage above the flume. Flow depth d was controlled within the trapezoidal channel by an adjustable weir at its downstream end, and flow discharge Q was measured with a

DOI: 10.1002/esp

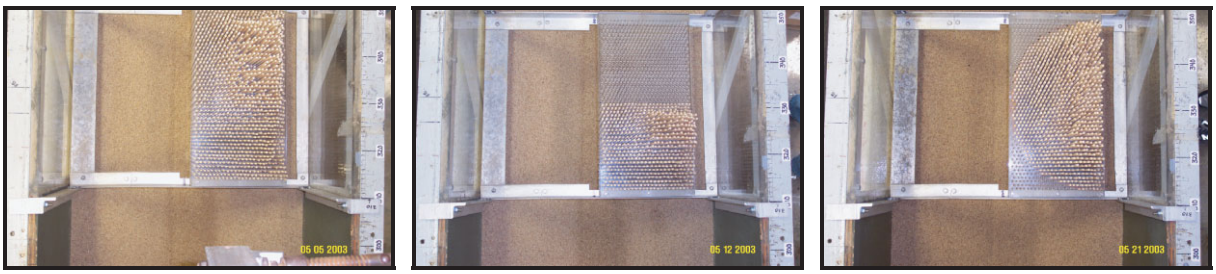

Figure 1. Photographs of the central vegetation zone showing the three different shapes used (rectangle on left, square in center and semicircle on right), the Plexiglas guide and aluminum frame suspended above the flume used to set the wooded dowels in a staggered arrangement and the dowels themselves. The vegetation densities shown are 11·53, 5·76 and 9·35 m^{-1}, respectively. Flow would be from bottom to top and flume width is 0·61 m. This figure is available in colour online at www.interscience.wiley.com/journal/espl

V-notch weir installed below the flume's overfall. Point gauges were used to measure flow depth, water surface elevation and channel dimensions.

Areas along this trapezoidal channel were populated with emergent, rigid vegetation. Wooden dowels with a diameter D_v of 5 mm were systematically planted into the channel bed at prescribed locations, overall shapes and packing densities. Using the model Q_B, a riffle-to-riffle spacing of 5–7 w, and $\lambda \approx 10\,w$ where λ is meander wavelength (see, e.g., Leopold *et al.*, 1960; Ackers and Charlton, 1970; Gregory *et al.*, 1994; Soar and Thorne, 2001), an equilibrium meander wavelength of 3 m was imposed on the channel and three vegetation zones were designated: two on the left-side of the channel spaced 3 m apart and one on the right-side of the channel spaced 1·5 m from the other two zones. Three vegetation shapes were used, each extending to the center of the channel (Figure 1): (1) a rectangle 0·5 m long; (2) a square 0·25 m long; and (3) a semicircle 0·5 m in diameter. As noted by Bennett *et al.* (2002), the semicircular shape was chosen to simulate a vegetated point bar whose radius was equal to half the channel width. The vegetation zone shapes were expanded to include a rectangle whose length was twice its width and a square, both of which also extended into the center of the channel.

These zones were populated with emergent wooden dowels placed in a staggered arrangement at relatively low, medium and high vegetation densities VD (m^{-1}) defined as the ratio of the frontal areas of the vegetation elements divided by the volume of water occupied over one meander wavelength, $\mathrm{VD} = 2mD_v d/d\lambda w$, where m is the number of dowels. A pre-drilled, double-layer Plexiglas guide suspended above the flume and mounted on an aluminum frame was used to plant individual vegetal elements into the prepared sand bed (Figure 1). Each 0·3 m long wooden dowel was pushed into the pre-wetted sand at the prescribed staggered density arrangement. The dowel spacing at the highest vegetation density was 9 mm. Lower vegetation densities were achieved by removing, at the same time, alternate rows of dowels and alternate dowels within the remaining rows. This ensured that all dowels were emergent with respect to Q_B and deeply seated within the channel boundary, and that geometric similarity of the vegetation pattern and the overall shape of the vegetation zone was independent of vegetation density.

The trapezoidal channel was reformed after each experiment, flow conditions were invariant between runs and the bed was digitized before and after each experiment with a laser microrelief system using a 2 mm by 5 mm grid with an effective vertical resolution equal to the bed material size. This laser was mounted on a computer-controlled positioning system suspended above the flume, and Figure 2 shows a typical digitized bed surface obtained after bed preparation and before a test run. The time length for each test run for each vegetation density was held constant, limited by the magnitude of bank erosion (stream channel expansion). All run times and vegetation densities are summarized in Table II.

Numerical model

Wu *et al.* (2005) developed a depth-averaged, two-dimensional numerical model to simulate flow, sediment transport and bed topography in mildly sinuous river channels with vegetation of various types. This model is based on the depth-integrated, Reynolds-averaged Navier–Stokes equations for shallow water flows as described by Wu and Wang (2004a, 2004b).

Although the model described by Wu *et al.* (2005) is applicable to a wide range of hydraulic and geomorphic conditions with bedload and suspended load transport of sediment mixtures and with various configurations and types

DOI: 10.1002/esp

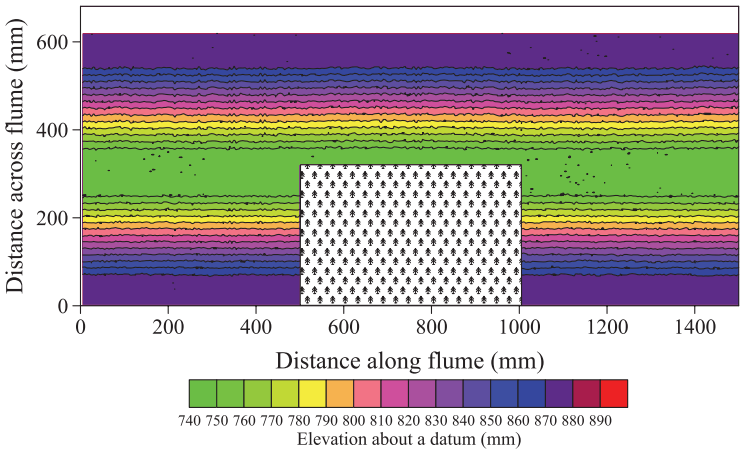

Figure 2. Contour map of the measured bed surface topography digitized using the laser microrelief system with the full vegetation zone in place. The spatial resolution of the measurement grid is 2 mm in the cross-stream and 5 mm in the downstream directions, and all data collected are shown without any post-processing. Flow would be from left to right. This figure is available in colour online at www.interscience.wiley.com/journal/espl

Table II. Summary of bulk hydraulic conditions at test section locations 250 and 750 mm at the conclusion of the experiment. Time refers to length of experiment, and NA means data are not available. All other parameters are defined in the text.

Vegetation Zone	Dowels per zone	Run			250 mm			750 mm		
		VD (m^{-1})	time (s)	*Sn*	*w* (m)	*d* (m)	*u* ($m\ s^{-1}$)	*w* (m)	*d* (m)	*u* ($m\ s^{-1}$)
None	0	0	–	1·00	0·330	0·050	0·200	0·330	0·050	0·200
Rectangle	78	0·77	14 400	1·00	0·360	0·051	0·180	0·336	0·052	0·189
	300	2·94	6 600	1·03	NA	NA	NA	NA	NA	NA
	1176	11·53	900	1·04	NA	NA	NA	NA	NA	NA
Square	39	0·38	14 400	1·01	0·340	0·042	0·231	0·356	0·054	0·172
	150	1·47	6 600	1·02	0·380	0·039	0·223	0·411	0·053	0·151
	588	5·76	900	1·03	0·358	0·046	0·200	0·424	0·052	0·150
Semicircle	62	0·61	14 400	1·00	0·346	0·040	0·238	0·327	0·053	0·190
	245	2·40	6 600	1·02	0·390	0·042	0·201	0·378	0·051	0·171
	954	9·35	900	1·02	0·350	0·045	0·210	0·401	0·059	0·139

of vegetation, here the discussion is restricted to mildly curved channels with emergent vegetation and dominated by bedload sediment transport of a single sediment size. Thus, the governing equations are

$$\frac{\partial[\rho(1-c)d]}{\partial t} + \frac{\partial[\rho(1-c)dU_i]}{\partial x_i} = 0 \tag{3}$$

$$\frac{\partial[\rho(1-c)dU_i]}{\partial t} + \frac{\partial[\rho(1-c)dU_iU_j]}{\partial x_i} = -\rho g(1-c)d\frac{\partial z_s}{\partial x_i} + \frac{\partial[(1-c)dT_{ij}]}{\partial x_i} + \frac{\partial D_{ij}}{\partial x_i} - (1-c)\tau_{bi} - f_{di}d \tag{4}$$

where t is time, x_i ($i = 1,2$) are the horizontal Cartesian coordinates, ρ is water density, d is flow depth, U_i is the depth-averaged flow velocity in the x_i direction, z_s is water surface elevation, c is the fractional vegetation density (defined as the ratio of the volume of vegetation to the total volume of water plus vegetation at the flow depth), T_{ij} ($j = 1,2$) are the depth-averaged turbulence stresses, D_{ij} are the dispersion terms due to the effect of secondary flow, f_{di} is the x_i component of the drag force exerted on the vegetation per unit volume and τ_{bi} is the x_i component of the bed shear stress.

Both Lane (1998) and Lane *et al.* (1999) discuss the importance of addressing the dispersion terms in the depth-averaged forms of the Navier–Stokes momentum equations (Equation (4)), especially in meandering river channels or at river confluences. Those 2D, depth-averaged models that address the dispersion terms, empirically, conceptually or analytically (see Lane, 1998), are superior in their predictive abilities as compared with those 2D models that ignore

DOI: 10.1002/esp

this phenomenon. The dispersion terms in Equation (4) are determined herein using the algebraic equations of Wu and Wang (2004b), who showed that this formulation can accurately simulate depth-averaged flow, bed and water surface topography and bed surface sorting patterns in a wide range of experimental and natural river meanders. The turbulent stress terms in Equation (4) are calculated with the aid of a depth-averaged $k-\varepsilon$ model employing the Boussinesq assumption and transport equations as described by Wu *et al.* (2005), where k is turbulent kinetic energy and ε is turbulence dissipation rate. It is noted that the standard $k-\varepsilon$ model as used here cannot simulate the turbulence generated by secondary circulation.

The drag force $\boldsymbol{f}_d$ exerted on vegetation per unit volume is given by

$$\boldsymbol{f}_d = \frac{1}{2} C_D \rho A \left| \bar{U}_v \right| \boldsymbol{U}_v = C_D \rho \alpha_v \frac{2c}{\pi D_e} \left| \bar{U}_v \right| \boldsymbol{U}_v \tag{5}$$

where C_D is the drag coefficient, A is the projected area of the vegetation in the streamwise direction per unit volume (taken as $4\alpha_v c/\pi D_v$), α_v is a shape factor that can account for the irregularity of vegetation ($\alpha_v = 1$ for a rigid cylinder) and $\bar{U}_v$ is the resultant flow velocity acting on the vegetation. For emergent vegetation, $\bar{U}_v$ in Equation (5) should be the depth-averaged downstream flow velocity U (Tsujimoto, 1998; Wu and Wang, 2004a). For emergent vegetation, the bed shear stress $\boldsymbol{\tau}_b$ is determined by

$$\boldsymbol{\tau}_b = \rho \frac{g n^2}{R_s^{1/3}} |U| \boldsymbol{U} \tag{6}$$

where n is the Manning roughness coefficient, R_s is the spacing hydraulic radius defined as $R_s = d b_v/(2d + b_v)$ and b_v is the spacing of the vegetation (Barfield *et al.*, 1979).

Bedload transport within the channel reach, herein written for a single grain size, is determined by

$$\frac{\partial[(1-c)\delta \bar{s}_b]}{\partial t} + \frac{\partial[\alpha_{bi}(1-c) q_b]}{\partial x_i} + \frac{1}{L_b}(1-c)(q_b - q_{b*}) = 0 \tag{7}$$

where $\bar{s}_b$ is the average concentration of bedload in the bedload zone of thickness δ, α_{bi} is the direction cosines of bedload movement, q_b is bedload transport rate (in $m^2\ s^{-1}$), q_{b*} is the bedload transport capacity or the bedload transport rate under equilibrium conditions and L_b is the non-equilibrium adaptation length of total load (a characteristic length for the sediment to adjust from a non-equilibrium state to the equilibrium state). Detailed discussions of L_b and its determination are presented by Wu (2004). Thus, erosion and deposition, assuming bedload transport of a single grain size, are determined from

$$(1-\phi)\left(\frac{\partial z_b}{\partial t}\right) = \frac{1}{L}(q_b - q_{b*}) \tag{8}$$

where z_b and ϕ are the elevation and porosity of the bed. For equilibrium transport, $q_b = q_{b*}$, and the equilibrium bed load transport rate q_{b*} is determined using the approach of Wu *et al.* (2000).

Equations (3), (4), (7) and (8) are the resulting governing equations, and Equations (5) and (6) with the formula of Wu *et al.* (2000) for q_{b*} yield the ancillary algorithms needed to complete the model. Additional discussion of boundary conditions and numerical solution methods can be found in the work of Wu *et al.* (2005). Extensive comparison of this numerical framework with datasets collected in experimental and natural river bends was conducted by Wu and Wang (2004b), Wu (2004) and Wu *et al.* (2005). In these studies, various components of the model were shown to agree well with observations of depth-averaged velocity, Reynolds stress and water surface topography, and the erosion, transport and deposition of unisize and mixed-size sediment in straight and meandering channels with and without vegetation.

Results

Channel adjustment to vegetation: Physical model

Response of the stable, trapezoidal channel to the introduction of emergent, rigid vegetation depends upon the shape of the vegetation zone and the density of the vegetation. In all cases, the added vegetation causes bank erosion and channel widening opposite and downstream from the vegetation zone and sediment deposition within the mid-channel regions upstream and downstream of the vegetation zones.

DOI: 10.1002/esp

These effects can be seen from the topographic maps for the rectangular vegetation zone (Figure 3). Marked channel expansion occurs downstream and opposite the introduced vegetation zone in the form of bank toe erosion and bank failure (Figure 3(c)). Since flow stage is just below the threshold of sediment motion, this eroded and failed bank material is quickly deposited within the lower confines of the channel, and a migrating aggradational front is present in the mid-channel region upstream of the vegetation zone (see spatial coordinate $x = 200$ mm and $y = 275$ mm, herein denoted as [200,275], Figure 3(c)). As vegetation density increases, the magnitudes of bank erosion, channel widening and mid-channel aggradation increase. The greatest amount of bank erosion and channel widening occurs directly opposite and just downstream of the trailing edge of the vegetation zone. Given enough time, these zones of

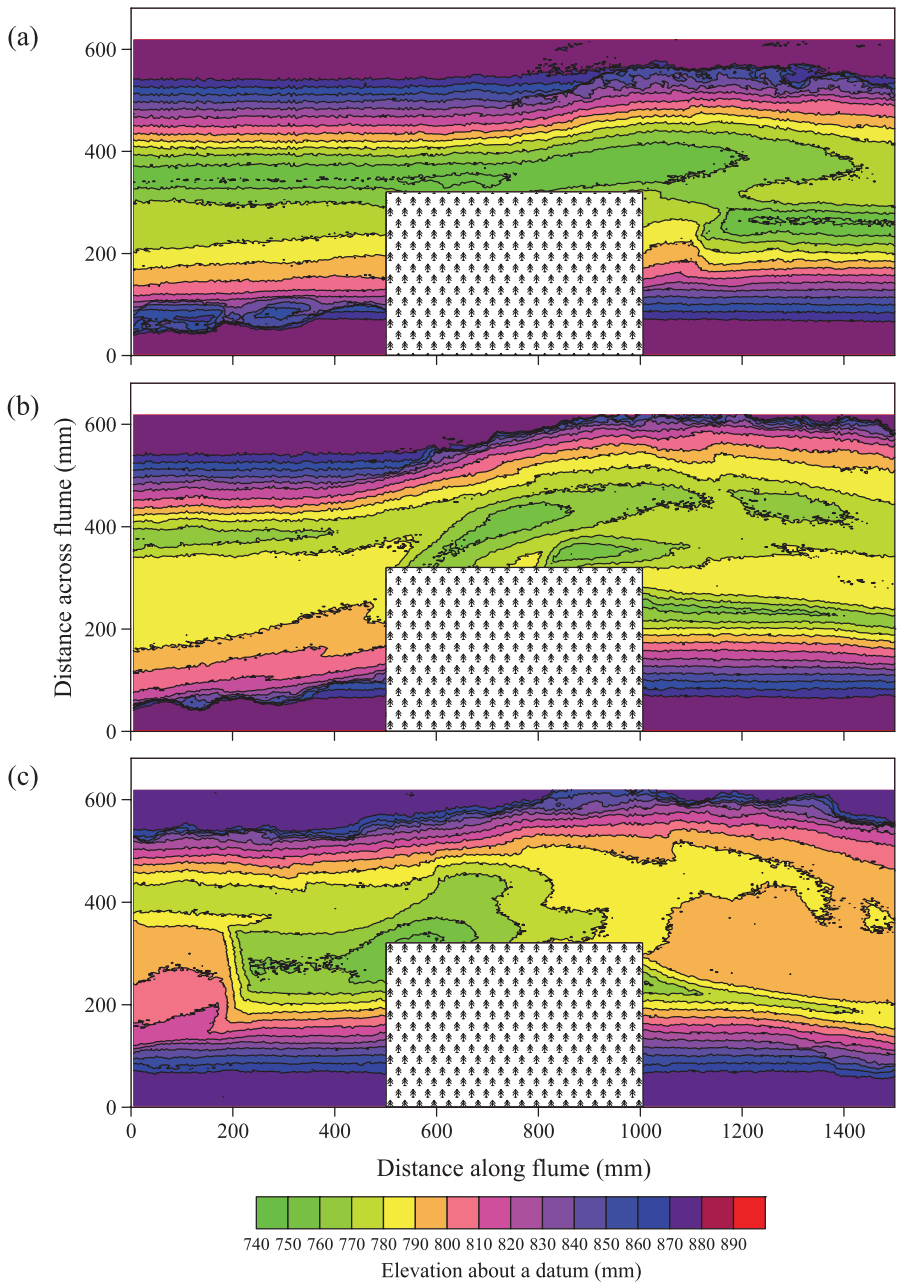

Figure 3. Contour maps of the measured bed surface topography for the rectangular vegetation zone with densities of (a) 0·77, (b) 2·94 and (c) 11·53 m^{-1} after run times listed in Table II. Flow is left to right. This figure is available in colour online at www.interscience.wiley.com/journal/espl

DOI: 10.1002/esp

degradation migrate downstream, encroaching the next vegetation zone on the opposite bank, as shown in Figure 3(a) and (b) in the range $0 < x < 400$.

Similar morphologic adjustments are observed for the square (Figure 4) and semicircular (Figure 5) vegetation zones. Both bank erosion and channel widening occur opposite and downstream of the vegetation zone, and this eroded bank material is deposited within the mid-channel regions of the stream corridor. Given enough time, these zones of bank erosion also migrate downstream, removing material just upstream of the vegetation zones (see Figures 4(c) and 5(c)).

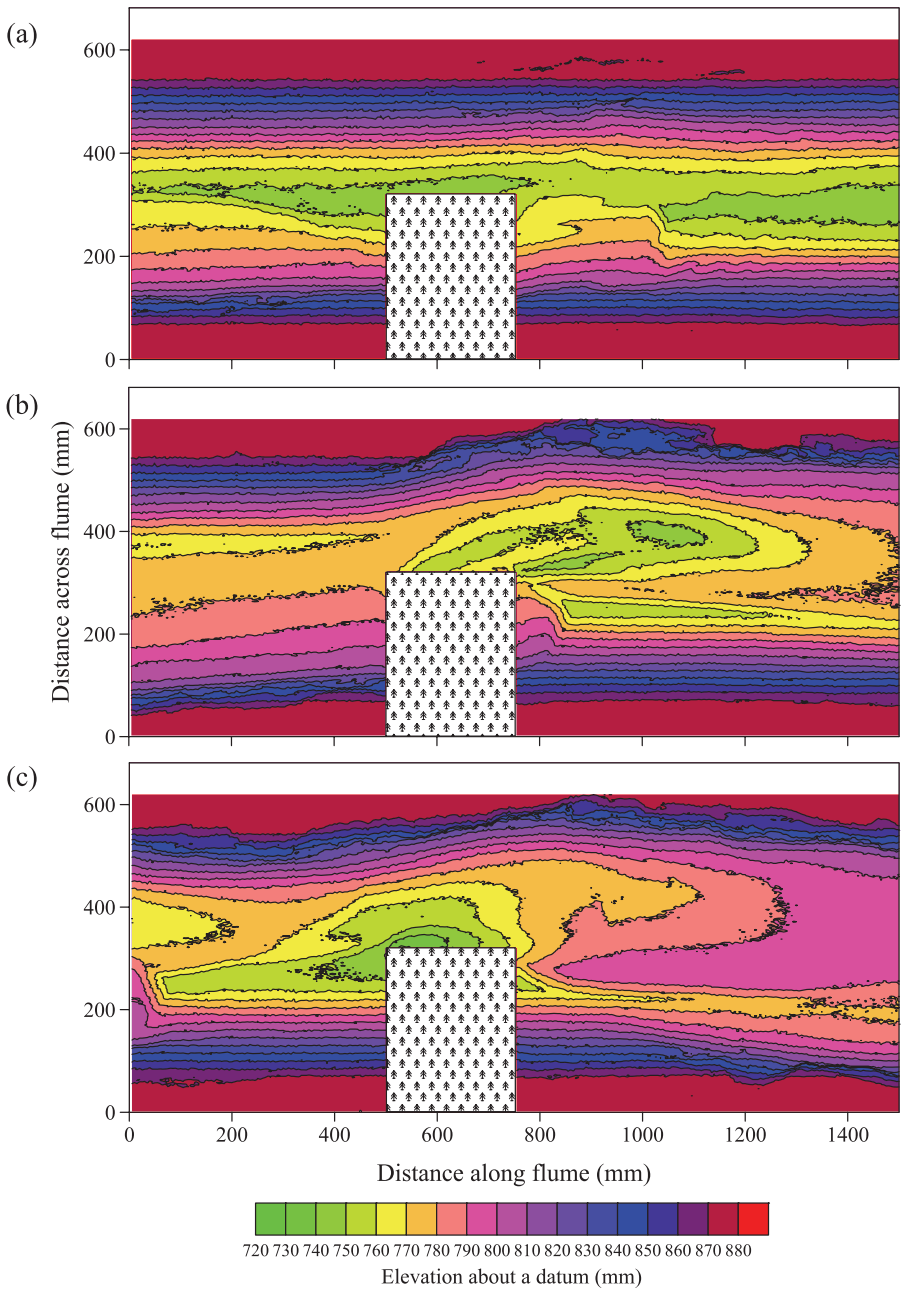

Figure 4. Contour maps of the measured bed surface topography for the square vegetation zone with densities of (a) 0·38, (b) 1·47 and (c) 5·76 m^{-1} after run times listed in Table II. Flow is left to right. This figure is available in colour online at www.interscience.wiley.com/journal/espl

DOI: 10.1002/esp

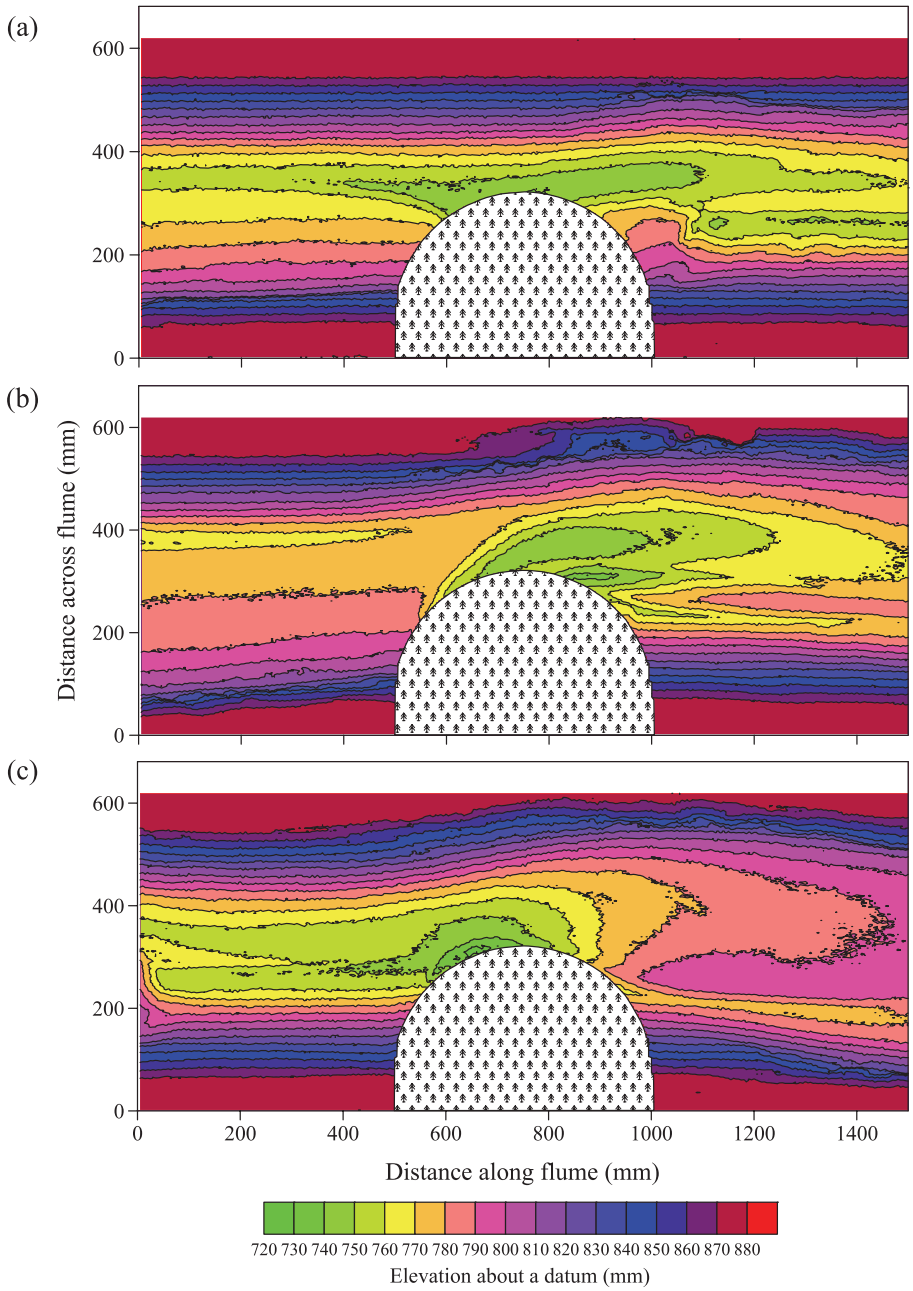

Figure 5. Contour maps of the measured bed surface topography for the semicircular vegetation zone with densities of (a) 0·61, (b) 2·40 and (c) 9·35 m^{-1} after run times listed in Table II. Flow is left to right. This figure is available in colour online at www.interscience.wiley.com/journal/espl

Localized scour holes are observed in two distinct geomorphic locations depending upon the length of the experiment. During the briefest experiments, which have the highest rates of erosion, scour hole development is restricted to the leading edge of and in close proximity to the vegetation zone (see Figures 3(c), 4(c) and 5(c)), whereas during the longest experiments, which are not nearly the most erosive conditions, scour holes develop opposite and just downstream of the vegetation zones, restricted in space to the trailing edge (wake) of these vegetal stands (see Figures 3(b), 4(b) and 5(b)). Presumably, these upstream, leading edge scour holes would be filled by the migrating aggradation fronts from upstream bank erosion and channel widening, whereas the downstream scour holes would need additional time for development.

DOI: 10.1002/esp

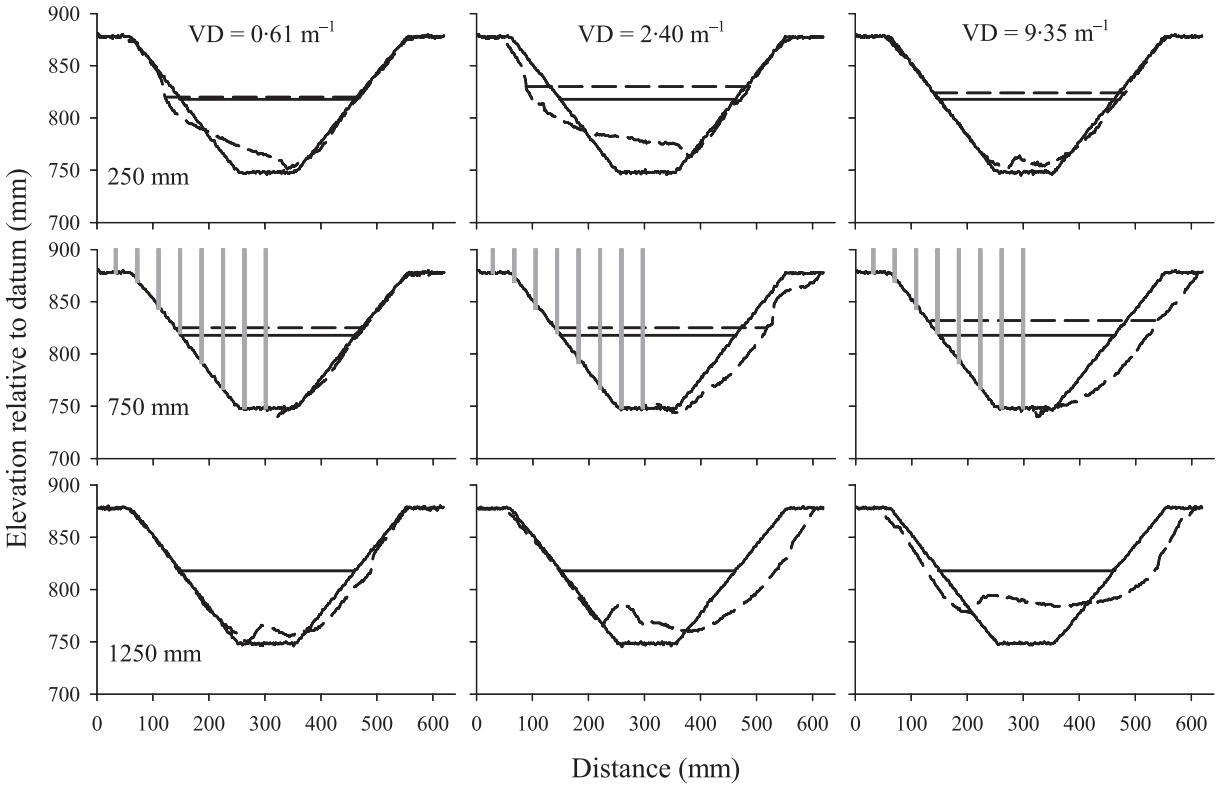

Figure 6. Bed and water surface profiles measured at beginning (solid line) and end (dashed line) of the experiment for the semicircular vegetation run. These cross-sections were taken at 250 (upper plots), 750 (middle plots) and 1250 mm (lower plots) along the flume for three different values of vegetation density VD. Vertical gray bars show the location of the vegetation. Perspective is looking upstream.

The channel adjustments to vegetation can be further quantified at a station. Three cross-sections can be defined at 250, 750 and 1250 mm downstream of the study reach, thus representing just upstream, the apex and just downstream of the vegetation zone. Bed and water surface profiles at these locations are shown in Figure 6 for the semicircular vegetation zone (the cross-sections for the rectangular and square vegetation zones look nearly the same as these). At $x = 250$ mm for relatively long experiment runs times (lower VD), the channel displays strongly asymmetric cross-sections due to selective near-bank erosion and near-bank and bed deposition. At $x = 750$ mm, only bank erosion is observed opposite the vegetation zone. At $x = 1250$ mm, the magnitude of mid-channel deposition and bank erosion increases with vegetation density. Moreover, depositional ridges (local topographic peaks) occur in the wake region of the vegetation zones. Using these observations, the cross-sections at $x = 250$ mm increase in channel width (by up to 19%), decrease in channel depth (by up to −22%) and increase in channel velocity (by up to 19%) at a station in response to the added vegetation (Figure 6, Table II). The cross-sections at $x = 750$ mm increase in channel width (by up to 28%) and channel depth (by up to 18%), and decrease in channel velocity (by up to −30%) at a station in response to the added vegetation (Figure 6, Table II).

The channel bed thalweg can be defined as the loci of all cross-sectional points where the bed elevation is at a minimum, and the thalweg sinuosity *Sn* is the distance measured along the thalweg divided by the distance along the streamwise axis. Figure 7 shows the smoothed loci of the maximum channel depth for each vegetation shape and density. These data show that thalweg sinuosity increases with vegetation density. Moreover, the thalweg bends toward the leading edge of the vegetation zone, intersecting each zone of the upstream side, and then bends away from the vegetation zone on its downstream side for higher values of VD. The most severe downstream wandering of the thalweg occurs for the rectangular vegetation zone at the highest values of VD. Thalweg sinuosity *Sn* is not markedly different from unity at the lowest values of VD (Table II). It is noted that slightly different values of *Sn* would be obtained if the top bank position or the location of the maximum flow velocity had been used instead of the loci of maximum flow depth.

DOI: 10.1002/esp

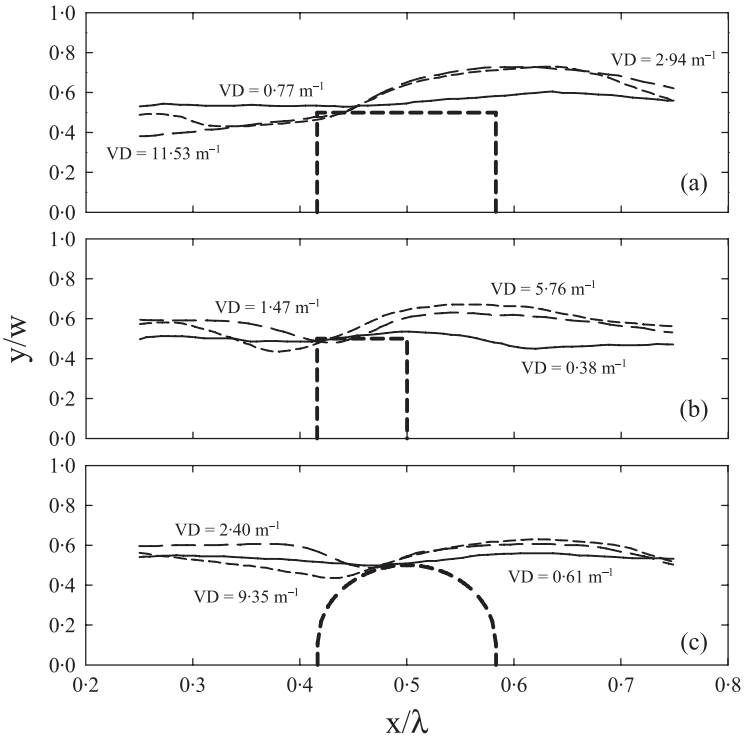

Figure 7. Loci of maximum flow depths for the (a) rectangular, (b) square and (c) semicircular vegetation zone as a function of vegetation density VD. Cross-stream and downstream distances (y and x) are normalized by flume width w and meander wavelength λ, respectively. Flow is left to right.

In general, the introduced vegetation causes the expansion of the channel width and an increase in channel sinuosity through bank erosion and thalweg meandering. This failed bank material, coupled with the sediment liberated from the near-vegetation scour hole, creates a downstream migrating aggradational front. This sediment flux can not exit the flume due to the imposed experimental conditions, i.e., the original bed is near threshold conditions, and a similar effect of channel scour and downstream deposition was observed by Wallerstein *et al.* (2001) in response to large woody debris. As the current channel expands and its thalweg meanders, in-channel deposition occurs upstream and downstream of the vegetation zones, creating a riffle or cross-over region, and in-channel erosion creates a pool or scour hole opposite and just downstream of the vegetation zone.

Channel adjustment to vegetation: Numerical model

The following conditions were imposed in the numerical model for comparison with these experimental data. A rectangular computational grid of variable density was used, with 131 grid lines along the flume (downstream direction) and 41 grid lines across the flume (transverse direction). The grid spacing near the vegetation ($\Delta x = 0{\cdot}025$ m and $\Delta y = 0{\cdot}016$ m) was finer than away from these locations ($\Delta x = 0{\cdot}040$ m and $\Delta y = 0{\cdot}016$ m). The computational time-step was 5 s, and each simulation lasted 6600 s. Manning's roughness coefficient n was 0·028, which produced the correct uniform flow conditions within the channel prior to vegetation planting, the vegetation drag coefficient C_D was 2·0, which was used as a calibrating input parameter, and the vegetation shape factor α_v was 1·0. Experimentally derived values of C_D for vegetation stands can range from 0·8 to 3·5, but typically vary from 1 to 1·5 (Garcia *et al.*, 2004). Higher values of C_D can be associated with cylinder orientation, blockage, relative submergence and wave drag effects (Wallerstein *et al.*, 2002; Alonso, 2004). In this application, bank sideslopes were near the angle of repose, yet the flow did not reach the top width of the channel. Any steepening of the banks above this angle due to fluvial erosion resulted in bank failure, and this failed material was added to the toe of the slope, ensuring that sediment mass was conserved. Additional modeling parameters were chosen following Wu (2004), Wu and Wang (2004b) and Wu *et al.* (2005).

DOI: 10.1002/esp

Figures 8 and 9 compare the changes in bed surface topography in response to the rectangular and semicircular vegetation zones for VD = 2·94 and VD = 2·40 m^{-1}, respectively, as observed in the experiment and as predicted by the model. In both test cases, the numerical model simulates quite well the pattern of net erosion and deposition in response to the introduced vegetation. For the rectangular vegetation zone, the magnitude and spatial extent of the bank erosion channel widening is simulated well (Figure 8), yet in the mid-channel regions slightly more deposition is observed upstream of the vegetation zone than is simulated, and less deposition is observed downstream of the vegetation zone than is simulated. In direct comparison of each grid node, the root-mean-square (rms) of the difference in elevation between the observation z_o and the prediction z_p can be defined as

$$\text{rms} = \sqrt{\frac{1}{m}(z_o - z_p)^2} \tag{9}$$

where m is the number of observations. For this simulation, rms = 19 mm, with 43 and 70% of the predictions falling within ±10 and ±20 mm, respectively, of the observations. This rms value is 28% when scaled by d, and 6% when scaled by w_T of the original channel.

For the semicircular vegetation zone, the model correctly simulates the general pattern of erosion and deposition in response to the introduced vegetation (Figure 9). In the bank erosion and widened region opposite the vegetation zone, lower but more spatially extensive erosion is simulated by the model as compared with the observations. Conversely, in the mid-channel regions, greater but more spatially restrictive deposition is simulated by the model as compared

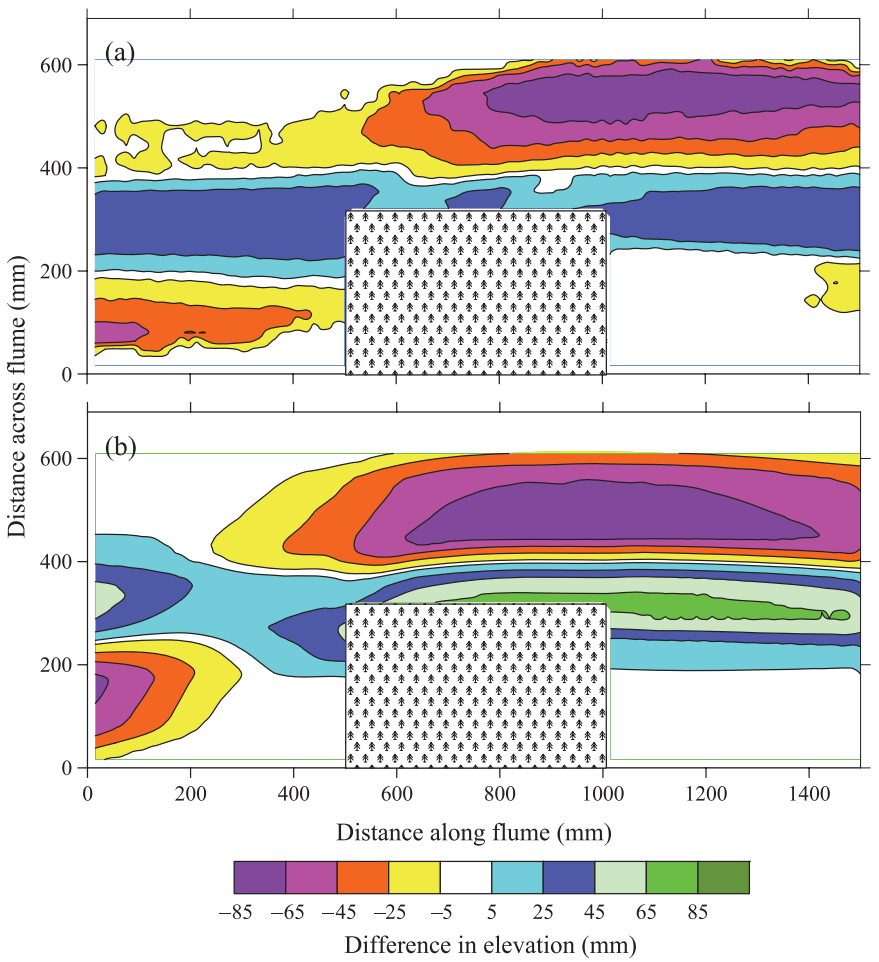

Figure 8. Contour plots of changes in bed surface topography in response to the rectangular vegetation zone with VD = 2·94 m^{-1} as (a) observed in the experiment and (b) predicted using the numerical model. Flow is left to right. This figure is available in colour online at www.interscience.wiley.com/journal/espl

DOI: 10.1002/esp

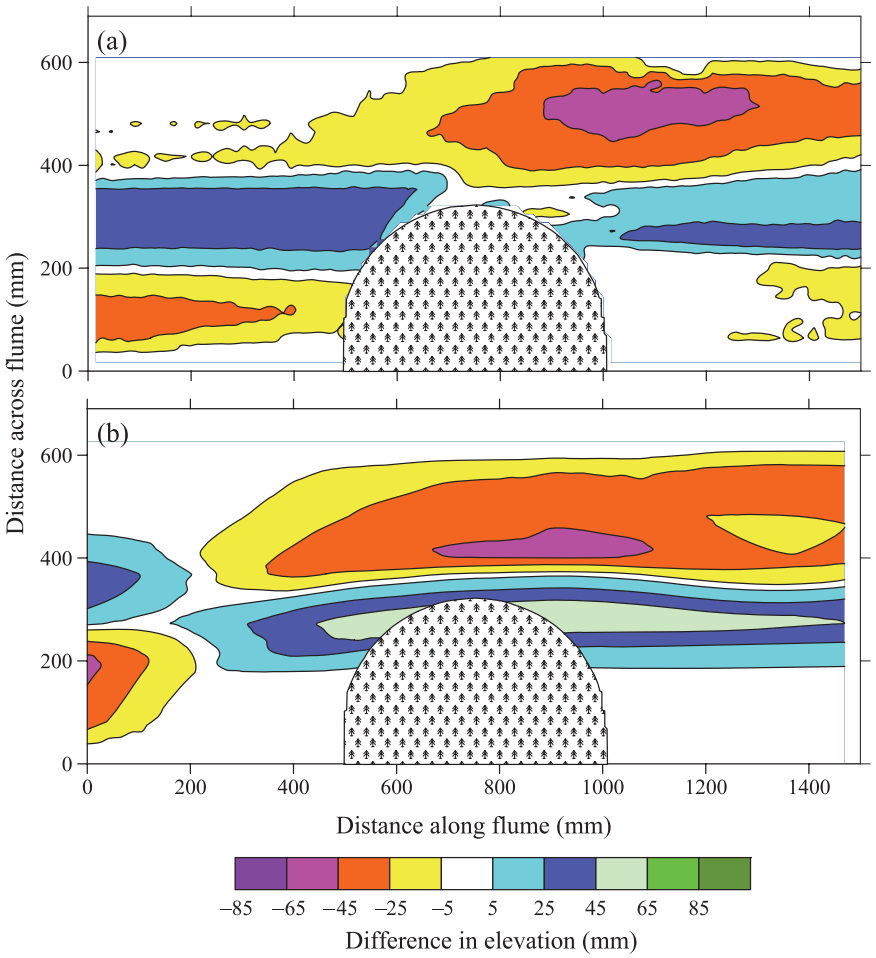

Figure 9. Contour plots of changes in bed surface topography in response to the semicircular vegetation zone with VD = 2·40 m^{-1} as (a) observed in the experiment and (b) predicted using the numerical model. Flow is left to right. This figure is available in colour online at www.interscience.wiley.com/journal/espl

with the observations. In direct comparison of each grid node, the rms of the difference between the observed and predicted elevations is 17 mm, with 49 and 78% of the predicted values falling within ±10 and ±20 mm, respectively, of the observed values. This rms value is 25% when scaled by d, and 5% when scaled by w_T of the original channel.

In summary, the overall adjustment of the stream channel to the added vegetation can be simulated correctly using the numerical model of Wu *et al.* (2005). The magnitude of channel erosion is predicted reasonably well, and the magnitude of deposition is somewhat over-predicted.

Discussion

Channel adjustment to vegetation: Physical processes of change

Whilst the effects of introducing vegetation to the physical model are significant, no quantitative measurements of the flow were made. As such, it is impossible to explain in mechanical terms the physical processes causing the observed localized erosion and deposition. Since the numerical model performed well in simulating channel adjustment to vegetation in the physical model, it will be used here to further examine the physical processes driving channel adjustment to vegetation. The simulation results for only the rectangular vegetation zone with VD = 2·94 m^{-1} will be presented for illustrative purposes. Varying the shape of the vegetation zone or the vegetation density would only alter the general characteristics and magnitude of these adjustments.

DOI: 10.1002/esp

The depth-averaged flow vectors for the unvegetated channel shows steady, uniform flow conditions and parabolic cross-stream velocity distributions, as expected, with near-bank downstream velocities U_1 near 0·11 m s^{-1} (at $y = 187$ mm) and increasing to 0·26 m s^{-1} in the center of the channel (at $y = 321$ mm, Figure 10(a)). By definition, the location of the maximum flow velocity is along the channel centerline and the channel velocity thalweg sinuosity *Sn*, based on the loci of maximum velocity, is unity. The introduction of vegetation to this flow causes an immediate alteration of the velocity vector field. Flow within the vegetation zone is greatly decelerated as compared with the unvegetated flow, reducing downstream velocities U_1 to 0·122 m s^{-1} at [703,253], and these decelerated velocities extend from the inner bank toward the channel center (Figure 10(b)). This component of flow velocity also tends to decrease from upstream to downstream within the vegetation zone, ranging from $U_1 = 0{\cdot}149$ m s^{-1} at [580,220] to $U_1 = 0{\cdot}092$ m s^{-1} at [899,220].

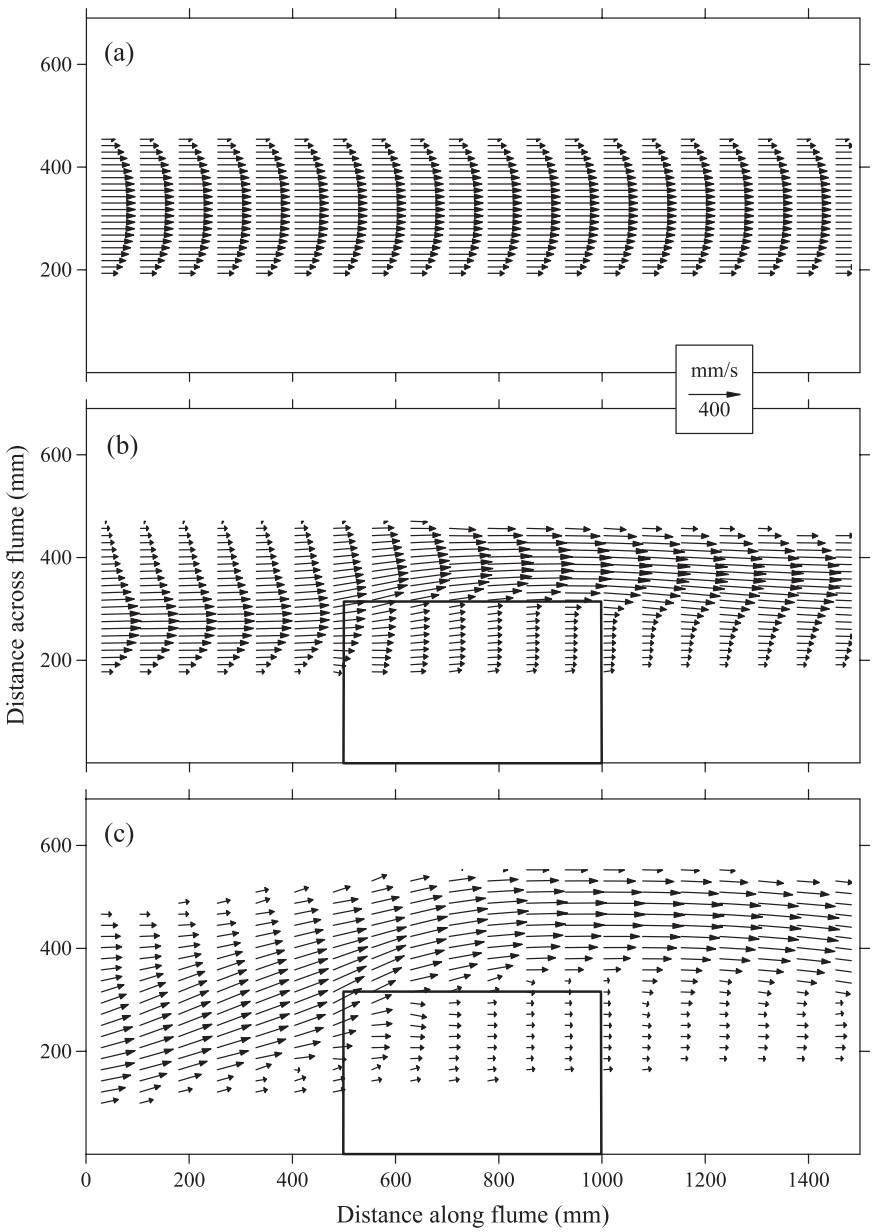

Figure 10. Simulated depth-averaged flow vectors for the trapezoidal channel with (a) no vegetation present, and in response to the rectangular vegetation zone (shown here as a lined box) at a density of 2·94 m^{-1} at (b) the beginning and (c) the conclusion of the experiment. Flow is left to right and a reference vector is shown. Only a small subset of the flow vectors is plotted.

DOI: 10.1002/esp

Flow within the channel, directly opposite the vegetation zone, is greatly accelerated as compared with the unvegetated channel flow, and this accelerated flow increases in velocity moving from upstream ($U_1 = 0{\cdot}296$ m s^{-1} at [581,354]) to downstream ($U_1 = 0{\cdot}372$ m s^{-1} at [899,388]; Figure 10(b)). Moreover, the once uniform flow vector field becomes strongly asymmetric along transverse channel cross-sections and strongly spatially varied along the channel length. The location of the maximum velocity now meanders as flow goes past the vegetation zone, moving away from the vegetation and toward the opposite bank. This deflection persists downstream until the flow field encounters the next vegetation zone, where this pattern then is shifted to the opposite bank (as evidenced by the entrance flow field at $x = 0$ mm). As channel adjustment proceeds with time, the flow field retains this meandering thalweg and flow accelerates and decelerates in response to the added flow resistance of the vegetation (Figure 10(c)). However, since the channel now has widened banks and is markedly more sinuous, the depth-averaged cross-stream velocity component U_2 increases to a maximum of about 0.1 m s^{-1} (e.g., $U_2 = 0{\cdot}127$ m s^{-1} at [507,321]; Figure 10(b)).

In response to the introduced vegetation, the distributions of bed shear stress $\boldsymbol{\tau}_b$ (Figure 11) parallel the flow vector field described above. For the unvegetated trapezoidal channel, as expected, bed shear stress is a maximum along the channel centerline, $\boldsymbol{\tau}_b = 1{\cdot}30$ Pa at $x = 321$ mm, decreasing toward the banks due to the changing bed topography and flow depth, and spatially invariant moving downstream along the channel due to flow uniformity (Figure 11(a)). The introduced vegetation markedly changes the distribution and magnitude of $\boldsymbol{\tau}_b$, and maximum shear stresses are observed opposite and just downstream of the vegetation zone ($\boldsymbol{\tau}_b = 2{\cdot}65$ Pa at [997,387], Figure 11(b)), which is significantly larger than the unvegetated trapezoidal channel. Moreover, the locus of maximum shear stress shifts from the vegetated bank upstream of the vegetation zone to the unvegetated bank at and downstream of the vegetation zone (Figure 11(b)). As channel adjustment ensues with time, the maximum bed shear stresses opposite and just downstream of the vegetation zone decrease in magnitude ($\boldsymbol{\tau}_b = 1{\cdot}12$ Pa at [997,387]), with new maximum values nearing 2·0 Pa ([1227,471]; Figure 11(c)). The maximum bed shear stresses upstream of the vegetation now are only moderately higher than their non-vegetated counterparts ($\boldsymbol{\tau}_b = 1{\cdot}64$ Pa at [358,270]), yet bed shear stresses within and just downstream of the vegetation zone remain relatively low, approaching near-zero values in places ($\boldsymbol{\tau}_b = 0{\cdot}09$ Pa at [997,203]). The meandering pattern of bed shear stress, a switching from the vegetated bank to the unvegetated bank, persists with time as the channel adjusts, but appears spatially continuous (less heterogeneous) along the bed (Figure 11(c)).

The driving mechanisms of river channel adjustment to in-stream, woody vegetation can now be discussed precisely. The introduced vegetation causes a localized increase in flow resistance, which markedly decelerates flow within and downstream of, and markedly accelerates and deflects flow around and away from, the vegetation zone. The accelerated flow causes localized increases in bed shear stress, which are both spatially discrete and significantly higher than those observed in the unvegetated trapezoidal channel. This accelerated flow and higher bed shear stress increases significantly bedload transport opposite and downstream of the vegetation zone and increases the hydraulic attack of this opposite stream bank. Channel bank erosion and widening ensue, and the thalweg of the main channel begins to meander. Over time, the sinuosity of the stream channel increases, and the locally high flow velocities and bed shear stresses diminish from their maxima and their distributions become less spatially discrete (more contiguous) along the channel boundary. The entrained sediment, as shown here, is deposited locally in the regions of relatively lower bed shear stress, forming bar complexes, riffles or cross-over regions, and pools and scour holes opposite and just downstream of the vegetation zone.

Using vegetation for stream corridor restoration

Given that managed plantings of emergent, woody vegetation cause thalweg meandering, asymmetric cross-sections and local pools and bars, and that vegetation provides corridors with a number of benefits to habitat and ecologic integrity, it holds that such actions could be adopted for restoring meandering channels within degraded or impaired stream corridors. A conceptual framework for stream restoration using vegetation is provided below. The following disclaimers are noted: (1) the corridor in question is nearly stable, as defined conceptually by Schumm *et al.* (1984), Simon and Hupp (1986) and Simon (1989), and localized erosion results in concomitant deposition; (2) a meandering planform is both geomorphically possible and environmentally desirable, such that a further decrease in slope will not cause channel unraveling and that an appreciable amount of bank erosion and channel widening in discrete locations is acceptable; (3) Q_B, rather than another flow frequency, is the channel-forming discharge; and (4) the choice of which tree species to plant can be determined, its survival rate is high regardless of species, hydrology and soil conditions, and natural colonization will occur (Webb and Erskine, 2003; Gurnell and Petts, 2006). Pezeshki and Shields (2006) note that survival statistics and growth rates of willow cuttings placed into degraded streams of Mississippi are maximized when soils contain less than 40% silt–clay content by mass and when the water table is more than 0·5–1·0 m below the soil surface during the growing season.

DOI: 10.1002/esp

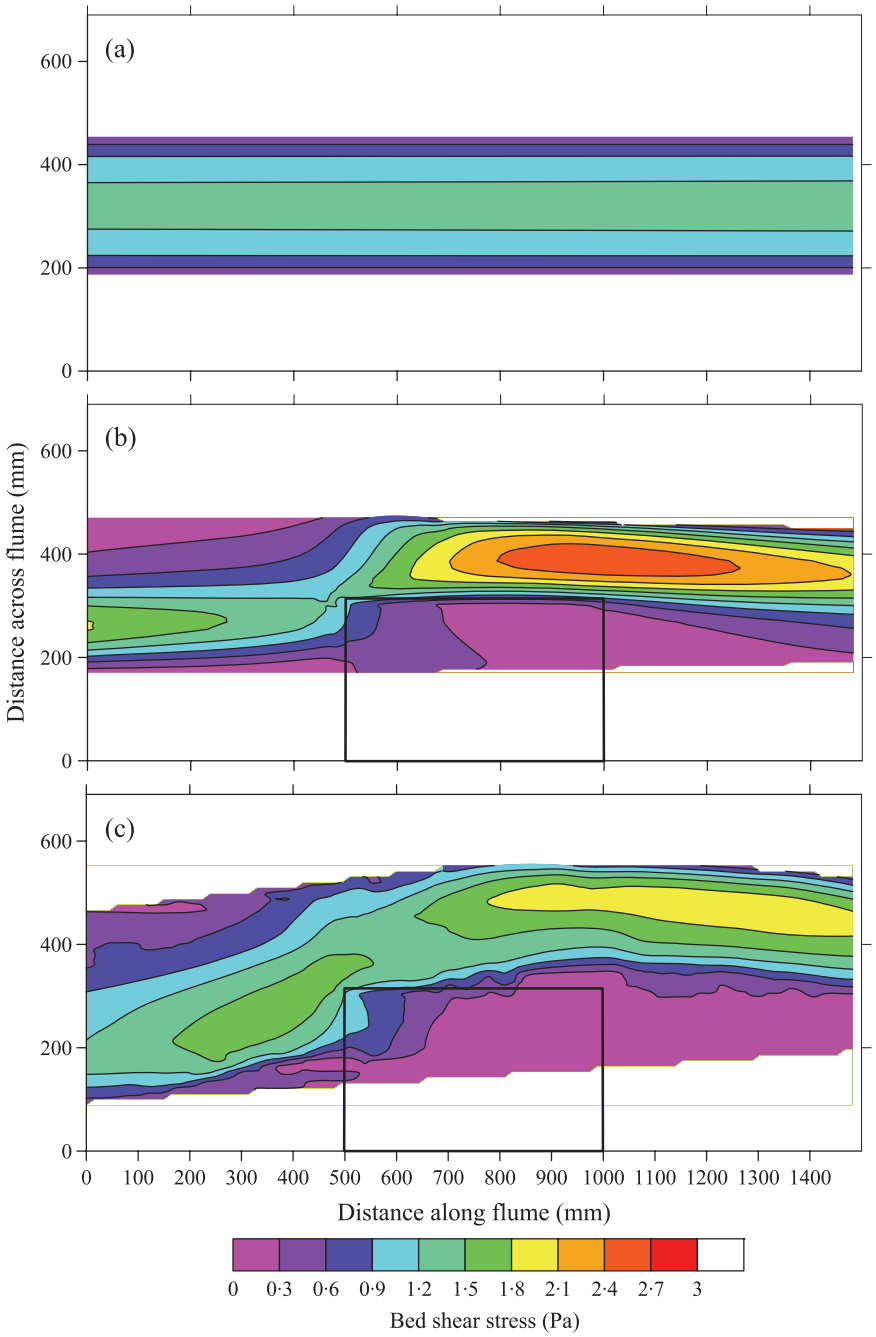

Figure 11. Contour plots of simulated distributions of bed shear stress for the trapezoidal channel with (a) no vegetation present, and in response to the rectangular vegetation zone (shown here as a lined box) at a density of 2·94 m^{-1} at (b) the beginning and (c) the conclusion of the experiment. Flow is left to right. This figure is available in colour online at www.interscience.wiley.com/journal/espl

Hasfurther (1985), Brookes (1987) and Soar and Thorne (2001) discuss in detail various approaches for the design of stable meandering planforms for use in stream corridor restoration. The primary methods are (1) the carbon copy technique, which seeks to replace meanders at a given locale with those prior to channel disturbance or instability; (2) employment of empirical relationships, which rely on locally or regionally derived predictive equations for channel dimensions; (3) the natural approach, which allows prevailing geomorphic processes to dictate channel adjustment and

DOI: 10.1002/esp

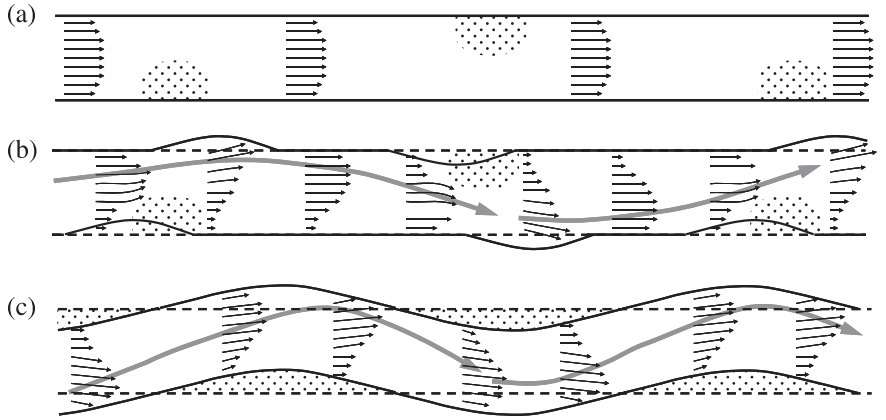

Figure 12. Schematic diagrams for stream channel response to managed plantings of emergent, woody vegetation showing (a) original stream corridor with planted vegetation (stippled regions), placed at prescribed meander wavelength, (b) initial response of the stream corridor to vegetation including flow deflection, toe erosion and bank failure opposite vegetation zones and deposition near and within vegetation zones and (c) ultimate meandering planform with vegetated point bars. Black arrows show generalized flow vectors, gray arrows show the location of maximum flow velocity and the dashed line shows the position of original stream corridor banks.

recovery; and (4) a systems approach, which considers the hydrologic and geomorphic characteristics of the entire catchment. Various practitioners have debated these approaches (Shields, 1996; Brookes and Sear, 1996), with recent attention focused on the applicability of empirical formulations (Rinaldi and Johnson, 1997a, 1997b).

The approach adopted here is a simple hybrid method that combines empiricism and natural geomorphic processes to evoke or trigger the desired effect, which in this case is a meandering planform with vegetated point bars as shown schematically in Figure 12. Keller (1978) was the first to suggest the manipulation of channel form, for the construction of pools and riffles, to initiate or induce erosion and deposition in desired locations along a stream corridor; others such as Downs and Thorne (2000; see also Hey, 1994) used in-stream structures to prompt the natural channel processes necessary to cause flow deflection and local scour and fill. First, an initial meander wavelength is determined based on Q_B using empirical or field data, with consideration of other geomorphic constraints including slope (e.g. Hey, 1994). Second, zones for vegetation plantings are identified within the stream corridor, fully cognizant that bank erosion and channel widening will occur on the opposite bank and that thalweg meandering will ensue. Third, woody vegetation is planted, such as willow posts (see, e.g., Watson *et al.*, 1997), at the prescribed intervals. The density of the vegetation should be sufficient to reduce near-bed shear stresses locally, and the size of the vegetation zone should be large enough to accelerate and deflect the main flow toward the opposing bank. Based on work presented here and by Bennett *et al.* (2002), VD should be of the order of 1–2 m^{-1}, the length of this vegetation zone should be about 1 w and its encroachment into the channel should be about 0.5 w. Values less than this may not cause the desired perturbation of the flow field. Once the vegetation is established, presumably over the first year or two, the vegetation will have a marked effect on local channel hydraulics. Flow deceleration will occur near and within the vegetation zones, inducing sediment deposition, further aggradation and stabilization of the point bar and natural colonization by indigenous vegetation. Concomitant flow acceleration and diversion around the vegetation will cause high bed shear stresses and velocities near the opposite stream bank, inducing bed and toe erosion, bank failure and channel widening (Figure 12). This eroded bed sediment and failed bank material, or some fractions thereof, will be deposited within and near the next vegetation zone downstream. This localized erosion and deposition, as triggered or forced by discrete plantings of vegetation, will cause the thalweg to meander at the approximate wavelength of the vegetation zones.

Over time, natural colonization of the point bars will occur, since vegetation will exploit such areas of low stream power (Hupp, 2000; Gurnell and Petts, 2006), the corridor will adopt a meandering planform and local erosion and deposition will attain a dynamic stability. It is assumed that some vegetation zones will stabilize, remain essentially intact and potentially anchor the meandering pattern over the short term, while others will be abandoned and subsumed at the sacrifice of planform development (Figure 12). Moreover, the final channel sinuosity may or may not be identical to the prescribed meander wavelength. This is of little consequence, since the desired effect – a meandering planform with vegetated point bars – is now in equilibrium with the prevailing hydrologic and geomorphic processes,

DOI: 10.1002/esp

and according to Wohl *et al.* (2005) restoration efforts with an acceptable range of variability in process seem more likely to succeed. Finally, the vegetation added to the river corridor will greatly enhance biodiversity in various ways and at a variety of scales as discussed by Wondzell and Bisson (2003).

Limitations of the physical model

It is duly noted that morphologic adjustment observed in physical models may not be entirely concordant with the field prototype. Because of necessary constraints imposed in construction, the model employed clear-water flows over an immobile sand bed. Abiaca Creek, at its prescribed channel forming discharge, would be transporting sediment over a completely mobile bed. Thus channel response would be modulated by the transport stage within the prototype. The model employed banks composed of sand near its angle of repose. Abiaca Creek would have composite banks made of sand, silt and clay of varying geotechnical characteristics. Thus bank stability criteria would be markedly different within the prototype. Moreover for the prototype, any failed bank material, especially the fine-grained sediments, would be transported out of the corridor rather than deposited near its source. Thus the relative amount of deposition observed in the physical model also may be markedly higher than would occur in the prototype. Finally, the model used very aggressive plantings of rigid, emergent vegetation, both large in diameter and height and high in density, and assuming high survival rates. Such plantings in natural settings, as well as a low mortality rate, may not be possible.

Nonetheless, the numerical model, given these imposed constraints, correctly simulates the overall magnitude and pattern of erosion and deposition within the physical model. Moreover, the numerical model provides in exact mechanical terms the physical processes driving river channel adjustment to in-stream, woody vegetation.

Conclusions

The motivation for the present work was to experimentally verify the transformation of a straight, degraded stream channel into a meandering, ecologically functional river corridor through the use of managed plantings of emergent, rigid vegetation, and to demonstrate, using a 2D, depth-averaged model, that the adjustment within the physical model can be simulated correctly and that the model then could be used to discuss these adjustments mechanistically. Whilst Bennett *et al.* (2002) showed that such thalweg meandering could be achieved in a fixed-wall flume using vegetation placed at equilibrium meander bend locations, the data presented herein show that planform meandering also can be achieved using a distorted Froude-scaled model in response to similar vegetation plantings. The magnitude of this channel response – bank erosion, pool and riffle development and increased channel sinuosity – depends upon the shape of the vegetation zone and the density of the vegetal elements, and these observations are verified with a recently developed numerical model.

Based on these results and those presented by Bennett *et al.* (2002), a hybrid method is suggested for the design of a meandering stream corridor using vegetation. For a design flow (bankfull), an equilibrium meander wavelength is derived using empirical methods, and dormant willow posts (or similar vegetation) are planted in a semicircular shape with a radius up to one-half the channel width. The vegetation should be planted in staggered arrangement at a vegetation density greater than 1.0 m^{-1} as averaged over one meander wavelength. Once planted and established, these vegetation stands will cause the development of scour pools and riffles and bank erosion at prescribed locations, resulting in thalweg meandering.

This hybrid technique should cost less than conventional construction designs, and work with and not against natural flow processes. Though the final channel planform may look markedly different from the original design, the stream corridor would be both stable and appropriate for the drainage system since it can freely adjust to the imposed temporal and spatial variations in boundary conditions and hydrology. Moreover, the numerical model developed by Wu *et al.* (2005), which has been successfully verified and validated with data here and elsewhere, could be employed as the primary tool for stream channel design and rehabilitation. Practitioners could use this model to explore the utility of vegetation, whether as willow plantings or large woody debris jams, in a variety of stream rehabilitation designs, thereby ensuring that the morphologic responses of the stream channel are in concert with the goals of the restoration program.

Acknowledgements

We thank Glenn Gray and Chris Francher for technical assistance during the mobile-bed experiments, and Mathias Römkens for use of the laser microrelief system. This research was financially supported by the USDA-CSREES NRI (2001-35102-10788) and USDA-ARS Specific Research Agreements 58-6408-2-0062 and 58-6408-3-0086.

DOI: 10.1002/esp

References

Abbe TB, Brooks AP, Montgomery DR. 2003. Wood in river rehabilitation and management. In *The Ecology and Management of Wood in World Rivers*, Gregory A, Boyer K, Gurnell A (eds). American Fisheries Society: Bethesda, MD, 367–389.

Ackers P, Charlton FG. 1970. The slope and resistance of small meandering channels. *Proceedings, The Institution of Civil Engineers*, Supplement 15 Paper 7362 S. London; 349–370.

Alonso CV. 2004. Transport mechanics of stream-borne logs. In *Riparian Vegetation and Fluvial Geomorphology*, Water Science and Application Series Volume 8, Bennett S, Simon A (eds). American Geophysical Union: Washington, DC; 59–69.

Barfield BJ, Tollner EW, Hayes JC. 1979. Filtration of sediment by simulated vegetation: I. Steady-state flow with homogenous sediment. *Transactions ASCE* **4451**: 540–556.

Bennett SJ, Pirim T, Barkdoll BD. 2002. Using simulated emergent vegetation to alter stream flow direction within a straight experimental channel. *Geomorphology* **44**:115–126.

Bennett SJ, Simon A (eds). 2004. *Riparian Vegetation and Fluvial Geomorphology*, Water Science and Application Series Volume 8. American Geophysical Union: Washington, DC.

Bernhardt ES, Palmer MA, Allan JD, Alexander G, Barnas K, Brooks S, Carr J, Clayton S, Dahm C, Follstad-Shah J, Galat D, Gloss S, Goodwin P, Hart D, Hassett B, Jenkinson R, Katz S, Kondolf GM, Lake PS, Lave R, Meyer JL, O'Donnell TK, Pagano L, Powell B, Sudduth E. 2005. Synthesizing U.S. river restoration efforts. *Science* **308**: 636–637.

Brookes A. 1987. Restoring the sinuosity of artificially straightened stream channels. *Environmental Geology and Water Science* **10**: 33–41.

Brookes A, Sear DA. 1996. Geomorphological principles for restoring channels. In *River Channel Restoration*, Brookes A, Shields FD Jr (eds). Wiley: Chichester; 75–101.

Downs PW, Thorne CR. 2000. Rehabilitation of a lowland river: reconciling flood defence with habitat diversity and geomorphological sustainability. *Journal of Environmental Management* **58**: 249–268.

Federal Interagency Stream Restoration Working Group (FISRWG). 1998. *Stream Corridor Restoration: Principles, Processes and Practices*. National Technical Information Service, US Department of Commerce: Springfield, VA.

García MH, López F, Dunn C, Alonso CV. 2004. Flow, turbulence, and resistance in a flume with simulated vegetation. In *Riparian Vegetation and Fluvial Geomorphology*, Water Science and Application Series Volume 8, Bennett S, Simon A (eds). American Geophysical Union: Washington, DC; 11–27.

Gregory KJ, Gurnell AM, Hill CT, Tooth S. 1994. Stability of the pool–riffle sequence in changing river channels. *Regulated Rivers: Research and Management* **9**: 35–43.

Gurnell A, Petts G. 2006. Trees as riparian engineers: the Tagliamento River, Italy. *Earth Surface Processes and Landforms* **31**: 1558–1574.

Gurnell AM, Van Oosterhout MP, De Vlieger B, Goodson JM. 2006. Reach-scale interactions between aquatic plants and physical habitat: River Frome, Dorset. *River Research and Applications* **22**: 667–680.

Hasfurther VR. 1985. The use of meander parameters in restoring hydrologic balance to reclaimed stream beds. In *The Restoration of River and Stream, Theories and Experience*, Gore JA (ed.). Butterworth: Boston, 21–40.

Henderson FM. 1966. *Open Channel Flow*, Macmillan: New York.

Hey RD. 1994. Environmentally sensitive river engineering. In *Rivers Handbook II*, Calow P, Petts GE (eds). Blackwell: Oxford; 337–362.

Hilderbrand RH, Watts AC, Randle AM. 2005. The myths of restoration ecology. *Ecology and Society* **10**: 19. http://www.ecologyandsociety.org/vol10/iss1/art19/ [17 August 2007].

Hupp CR. 2000. Hydrology, geomorphology and vegetation of Coastal Plain rivers in the south–eastern USA. *Hydrological Processes* **14**: 2991–3010.

Hupp CR, Osterkamp WR. 1996. Riparian vegetation and fluvial geomorphic processes. *Geomorphology* **14**: 277–295.

Hupp CR, Rinaldi M. 2007. Riparian vegetation patterns in relation to fluvial forms and channel evolution along selected rivers of Tuscany (central Italy). *Annals of the Association of American Geographers* **97**: 12–30.

Johnson WC. 2000. Tree recruitment and survival in rivers: influence of hydrological processes. *Hydrological Processes* **14**: 3051–3074.

Julien PY. 2002. *River Mechanics*. Cambridge University Press: Cambridge.

Keller EA. 1978. Pools, riffles, and channelization. *Environmental Geology* **2**: 119–127.

Lane SN. 1998. Hydraulic modelling in hydrology and geomorphology: a review of high resolution approaches. *Hydrological Processes* **12**: 1131–1150.

Lane SN, Bradbrook KF, Richards KS, Biron PA, Roy AG. 1999. The application of computational fluid dynamics to natural river channels: three-dimensional versus two-dimensional approaches. *Geomorphology* **29**: 1–20.

Leopold LB, Bagnold RA, Wolman RG, Brush LM. 1960. *Flow Resistance in Sinuous or Irregular Channels*, USGS Professional Paper 282-D, Washington, DC; 111–134.

López F, García M. 2001. Mean flow and turbulence structure of open-channel flow through non-emergent vegetation. *Journal of Hydraulic Engineering* **127**: 392–402.

Montgomery DR, Piégay H. 2003. Wood in rivers: interactions with channel morphology and processes. *Geomorphology* **51**: 1–5.

Nepf H, Vivoni E. 2000. Flow structure in depth-limited, vegetated flow. *Journal of Geophysical Research* **105**(C12): 28 547–28 557.

Palmer MA, Bernhardt ES. 2006. Hydroecology and river restoration: ripe for research and synthesis. *Water Resources Research* **42**: W03S07. DOI: 10.1029/2005WR004354

Palmer MA, Bernhardt ES, Allan JD, Lake PS, Alexander G, Brooks S, Carr J, Clayton S, Dahm CN, Follstad Shah J, Galat DL, Loss SG, Goodwin P, Hart DD, Hassett B, Jenkinson R, Katz S, Kondolf GM, Lave R, Meyer JL, O'Donnell TK, Pagano L, Sudduth E. 2005. Standards for ecologically successful river restoration. *Journal of Applied Ecology* **42**: 208–217.

Petryk S, Bosmajian G III. 1975. Analysis of flow through vegetation. *Journal of the Hydraulics Division ASCE* **101**: 871–884.
Pezeshki S, Shields FD Jr. 2006. Black willow cutting survival in streambank plantings, southeastern United States. *Journal of the American Water Resources Association* **42**: 191–200.
Piégay H, Bornette G, Citterio A, Hérouin E, Moulin B, Statiotis C. 2000. Channel instability as a control on silting dynamics and vegetation patterns within perifluvial aquatic zones. *Hydrological Processes* **14**: 3011–3029.
Rinaldi M, Johnson PA. 1997a. Characterization of stream meanders for stream restoration. *Journal of Hydraulic Engineering* **123**: 567–570.
Rinaldi M, Johnson PA. 1997b. Stream meander restoration. *Journal of the American Water Resources Association* **33**: 855–866.
Schumm SA, Harvey MD, Watson CC. 1984. *Incised Channels: Morphology, Dynamics and Control*. Water Resources: Littleton.
Shields FD Jr. 1996. Hydraulic and hydrologic stability. In *River Channel Restoration*, Brookes A, Shields FD Jr (eds). Wiley: Chichester; 23–74.
Shields FD Jr, Copeland RR, Klingeman PC, Doyle MW, Simon A. 2003. Design for stream restoration. *Journal of Hydraulic Engineering* **129**: 575–584.
Shields FD Jr, Knight SS, Cooper CM. 1995a. Use of the index of biotic integrity to assess physical habitat degradation in warmwater streams. *Hydrobiologia* **312**: 191–208.
Shields FD Jr, Knight SS, Cooper CM. 1995b. Rehabilitation of watersheds with incising channels. *Water Resources Bulletin* **31**: 971–982.
Shields FD Jr, Morin N, Cooper CM. 2004. Large woody debris structures for sand-bed channels. *Journal of Hydraulic Engineering* **130**: 208–217.
Simon A. 1989. A model of channel response in disturbed alluvial channels. *Earth Surface Processes and Landforms* **14**: 11–26.
Simon A, Hupp C. 1986. Channel evolution in modified Tennessee channels. *Proceedings of the Fourth Federal Interagency Sedimentation Conference*. Government Printing Office: Washington, DC; 5-71–5-82.
Simon A, Rinaldi M. 2000. Channel instability in the loess area of the Midwestern United States. *Journal of the American Water Resources Association* **36**: 133–150.
Soar PJ, Thorne CR. 2001. *Channel Restoration Design for Meandering Rivers*, Final Report ERDC/CHL CR-01-1, Vicksburg, US Army Research and Development Center.
Thorne CR. 1999. Bank processes and channel evolution in the incised rivers of north-central Mississippi. In *Incised River Channels: Processes, Forms, and Management*, Darby SE, Simon A (eds). Wiley: Chichester; 97–121.
Tsujimoto T. 1998. Development of sand island with vegetation in fluvial fan river under degradation. In *Proceedings of Water Resources Engineering '98*, Vol. 1, Apt, SR (ed.). ASCE: Reston, VA, 574–579.
Tsujimoto T. 1999. Fluvial processes in streams with vegetation. *Journal of Hydraulic Engineering* **37**: 798–803.
US Department of Agriculture – Natural Resources Conservation Service (USDA-NRCS). 1996. *National Engineering Handbook Series, Part 650, Chap. 16, Streambank and Shoreline Protection*. US Government Printing Office: Washington, DC.
US Environmental Protection Agency (EPA). 2000a. *The Quality of Our Nation's Waters, a Summary of the National Water Quality Inventory: 1998 Report to Congress*, Report EPA841-S-00-001, Washington, DC.
US Environmental Protection Agency (EPA). 2000b. *Principles for the Ecological Restoration of Aquatic Resources*, Report EPA841-F-00-003, Office of Water (4501F), Washington, DC.
Wallerstein NP, Alonso CV, Bennett SJ, Thorne CR. 2001. Distorted Froude-scaled flume analysis of large woody debris. *Earth Surface Processes and Landforms* **26**: 1265–1283.
Wallerstein NP, Alonso CV, Bennett SJ, Thorne CR. 2002. Surface wave forces acting on submerged logs. *Journal of Hydraulic Engineering* **128**: 349–353.
Wallerstein NP, Thorne CR. 2004. Influence of large woody debris on morphological evolution of incised, sand-bed channels. *Geomorphology* **57**: 53–73.
Watson CC, Abt SR, Derrick D. 1997. Willow posts bank stabilization. *Journal of the American Water Resources Association* **33**: 293–300.
Webb AA, Erskine WD. 2003. A practical scientific approach to riparian vegetation rehabilitation in Australia. *Journal of Environmental Management* **68**: 329–341.
Wohl E, Angermeier PL, Bledsoe B, Kondolf GM, MacDonnell L, Merritt DM, Palmer MA, Poff NL, Tarboton D. 2005. River restoration. *Water Resources Research* **41**: W10301. DOI: 10.1029/2005WR003985
Wondzell SM, Bisson PA. 2003. Influence of wood on aquatic biodiversity. In *The Ecology and Management of Wood in World Rivers*, Gregory A, Boyer K, Gurnell A (eds). American Fisheries Society: Bethesda, MD: 249–263.
Wu W. 2004. Depth-averaged 2-D numerical modeling of unsteady flow and nonuniform sediment transport in open channels. *Journal of Hydraulic Engineering* **130**: 1013–1024.
Wu W, Shields FD Jr, Bennett SJ, Wang SSY. 2005. A depth-averaged 2-D model for flow, sediment transport and bed topography in curved channels with riparian vegetation. *Water Resources Research* **41**: W03015. DOI: 10.1029/2004WR003730
Wu W, Wang SSY. 2004a. Depth-averaged numerical modeling of flow and sediment transport in open channels with vegetation. In *Riparian Vegetation and Fluvial Geomorphology*, Water Science and Application Series Volume 8, Bennett SJ, Simon A (eds). American Geophysical Union: Washington, DC; 253–265.
Wu W, Wang SSY. 2004b. Depth-averaged 2-D calculation of flow and sediment transport in curved channels. *International Journal of Sediment Research* **19**: 241–257.
Wu W, Wang SSY, Jia Y. 2000. Nonuniform sediment transport in alluvial rivers. *Journal of Hydraulic Research* **38**: 427–434.